Proceedings of the ASME 2022 International Design Engineering Technical Conferences & Computers and Information in Engineering Conference
IDETC/CIE 2022
August 14 – 17, 2022, St. Louis, USA

DETC2022/DAC-89707

HIERARCHICAL DEEP GENERATIVE MODELS FOR DESIGN UNDER FREE-FORM GEOMETRIC UNCERTAINTY

Wei (Wayne) Chen
Dept. of Mechanical Engineering
Northwestern University
Evanston, IL 60208
wei.wayne.chen@northwestern.edu

Doksoo Lee
Dept. of Mechanical Engineering
Northwestern University
Evanston, IL 60208
dslee@u.northwestern.edu

Oluwaseyi Balogun
Dept. of Mechanical Engineering
Northwestern University
Evanston, IL 60208
o-balogun@northwestern.edu

Wei Chen*
Dept. of Mechanical Engineering
Northwestern University
Evanston, IL 60208
weichen@northwestern.edu

ABSTRACT

Deep generative models have demonstrated effectiveness in learning compact and expressive design representations that significantly improve geometric design optimization. However, these models do not consider the uncertainty introduced by manufacturing or fabrication. Past work that quantifies such uncertainty often makes simplifying assumptions on geometric variations, while the "real-world", "free-form" uncertainty and its impact on design performance are difficult to quantify due to the high dimensionality. To address this issue, we propose a Generative Adversarial Network-based Design under Uncertainty Framework (GAN-DUF), which contains a deep generative model that simultaneously learns a compact representation of nominal (ideal) designs and the conditional distribution of fabricated designs given any nominal design. This opens up new possibilities of 1) building a universal uncertainty quantification model compatible with both shape and topological designs, 2) modeling free-form geometric uncertainties without the need to make any assumptions on the distribution of geometric variability, and 3) allowing fast prediction of uncertainties for new nominal designs. We can combine the proposed deep generative model with robust design optimization or reliability-based design optimization for design under uncertainty. We demonstrated the framework on two real-world engineering design examples and showed its capability of finding the solution that possesses better performances after fabrication.

INTRODUCTION

Many engineering design problems boil down to geometric optimization. However, geometric optimization remains a grand challenge because of its extreme dimensional complexity and often hard-to-achieve performance objective. Recent work has shown that deep generative models can learn a compact and expressive design representation that remarkably improves geometric design optimization performances (indicated by both the quality of optimal solutions and the computational cost) [1, 2, 3]. However, past work based on deep generative models only considers the ideal scenario where manufacturing or fabrication imperfections do not occur, which is unrealistic due to the existence of uncertainties in reality, such as limited tool precision or wear. Such imperfections sometimes have a high impact on a design's

*Address all correspondence to this author.

performance or properties. Consequently, the originally optimal solution (obtained by only considering the ideal scenario) might not possess high performance or desired properties after fabrication.

Past work has developed task-specific robust optimization techniques to identify geometric design solutions that are insensitive to variations of load, materials, and geometry [4,5,6]. However, due to the lack of generalizable uncertainty representation that is compatible with different geometric representations, previous work often makes simplifying assumptions on geometric variations (*e.g.*, the distribution or the upper/lower bound of uncertain parameters), while the "real-world", "free-form" geometric uncertainty and its impact on design performance are difficult to quantify due to the high-dimensionality. In this paper, we propose a *Generative Adversarial Network-based Design under Uncertainty Framework (GAN-DUF)* to allow uncertainty quantification (UQ) of free-form geometric variability under real-world scenarios. The term "free-form" refers to two aspects: 1) the geometric variability has no shape or topological restrictions and 2) no assumption on the form of uncertainty is needed. Therefore, this framework is generalizable to any shape or topological designs. It improves existing geometric design under uncertainty from four aspects: 1) The generative adversarial network (GAN) uses a compact representation to reparameterize geometric designs, allowing accelerated optimization; 2) The GAN associates real-world, free-form fabrication uncertainty with ideal designs (*i.e.*, *nominal designs*) by learning a conditional distribution of fabricated designs given any nominal design; 3) The optimization process accounts for the distribution of geometric variability underlying any manufacturing processes, and allows UQ for robust design optimization or reliability-based design optimization; 4) The compact representation of nominal designs allows gradient-free global optimization due to the representation's low-dimensionality.

We list the contributions of this work as follows:

1. We propose a hierarchical deep generative model to simultaneously learn a compact representation of designs and quantify their real-world, free-form geometric uncertainties.
2. We combine the proposed model with a robust design optimization framework and demonstrate its effectiveness on two realistic robust design examples.
3. We build two benchmark datasets, containing nominal and fabricated designs, which will facilitate future study on data-driven design under manufacturing uncertainty.

BACKGROUND

In this section, we introduce Generative Adversarial Networks and design under uncertainty.

Generative Adversarial Networks

The generative adversarial network [7] models a game between a *generator* G and a *discriminator* D. The goal of G is to generate samples (designs in our case) that resemble those from data; while D tries to distinguish between real data and generated samples. Both models improve during training via the following minimax optimization:

$$\min_G \max_D V(D,G) = \mathbb{E}_{\mathbf{x}\sim P_{\text{data}}}[\log D(\mathbf{x})] + \mathbb{E}_{\mathbf{z}\sim P_{\mathbf{z}}}[\log(1-D(G(\mathbf{z})))], \tag{1}$$

where P_{data} is the data distribution and $\mathbf{z} \sim P_{\mathbf{z}}$ is the noise that serves as G's input. A trained generator thus can map from a predefined noise distribution to the distribution of designs. Due to the low dimensionality of $\mathbf{z}$, we can use it to more efficiently control the geometric variation of high-dimensional designs.

Despite the ability to generate high-dimensional data from low-dimensional noise, standard GANs do not have a way of regularizing the noise; so it usually cannot reflect an intuitive design variation, which is unfavorable in many design applications. To compensate for this weakness, the InfoGAN encourages interpretable and disentangled latent representations by adding the *latent codes* $\mathbf{c}$ as G's another input and maximizing the lower bound of the mutual information between $\mathbf{c}$ and $G(\mathbf{c},\mathbf{z})$ [8]. The mutual information lower bound L_I is

$$L_I(G,Q) = \mathbb{E}_{\mathbf{c}\sim P(\mathbf{c}),\mathbf{x}\sim G(\mathbf{c},\mathbf{z})}[\log Q(\mathbf{c}|\mathbf{x})] + H(\mathbf{c}), \tag{2}$$

where $H(\mathbf{c})$ is the entropy of the latent codes, and Q is the auxiliary distribution for approximating $P(\mathbf{c}|\mathbf{x})$. The InfoGAN's training objective becomes:

$$\min_{G,Q} \max_D \mathbb{E}_{\mathbf{x}\sim P_{\text{data}}}[\log D(\mathbf{x})] + \mathbb{E}_{\mathbf{c}\sim P_{\mathbf{c}},\mathbf{z}\sim P_{\mathbf{z}}}[\log(1-D(G(\mathbf{c},\mathbf{z})))] - \lambda L_I(G,Q), \tag{3}$$

where λ is a weight parameter. In practice, $H(\mathbf{c})$ is usually treated as a constant as $P_{\mathbf{c}}$ is fixed.

Since InfoGAN provides a interpretable and disentangled latent representation that is also compact and low-dimensional, searching for design solutions in this latent space is much more efficient than searching in the original high-dimensional design space [1,2,3]. Building on top of the InfoGAN model, this work proposes a new deep generative model that constructs a hierarchical latent representation to simultaneously model 1) the latent representation of nominal designs and 2) the distribution of fabricated designs conditioned on any nominal design.

Design under Uncertainty

Design under uncertainty aims to account for stochastic variations in engineering design to identify optimal designs that are robust and/or reliable under the variations associated with various sources (*e.g.*, material, geometry, and operating conditions) [9, 10]. Two common approaches are robust design optimization (RDO) [11] and reliability-based design optimization (RBDO) [12, 13].

The goal of RDO is to minimize the effects of variation without eliminating the sources of uncertainty [11]. RDO approaches simultaneously maximize the mean performance $\mu(C(\cdot))$ and minimize the variance of the performance $\sigma^2(C(\cdot))$ over random variables $\boldsymbol{\xi}$ representing the sources of uncertainty (*e.g.*, noise or control factor), where $C(\cdot)$ is the performance function. The design goal, in general, involves the following optimization problem :

$$\min_{\mathbf{x}} J(\mathbf{x}, \boldsymbol{\xi}) = F(\mu(C(\mathbf{x})), \sigma(C(\mathbf{x}))), \tag{4}$$

where $\mathbf{x}$ is the design variable, and F is the multi-objective cost function that is typically formulated as $F(\cdot) = \mu(\cdot) + k\sigma(\cdot)$ with k as the tuning parameter. $\mu(C(\cdot))$ and $\sigma^2(C(\cdot))$ are the statistical moments of the cost w.r.t. the associated uncertainty $\boldsymbol{\xi}$ and can be expressed as:

$$\begin{aligned} \mu(C(\mathbf{x})) &= \mathbb{E}_{\boldsymbol{\xi}}[C(\mathbf{x})] = \int_{\boldsymbol{\xi}} p(\boldsymbol{\xi}) C(\mathbf{x}))\, d\boldsymbol{\xi}, \\ \sigma^2(C(\mathbf{x})) &= \mathbb{E}_{\boldsymbol{\xi}}[[C(\mathbf{x}) - \mu(C(\mathbf{x})]^2] \\ &= \int_{\boldsymbol{\xi}} p(\boldsymbol{\xi})[C(\mathbf{x}) - \mu(C(\mathbf{x}))]^2\, d\boldsymbol{\xi}. \end{aligned} \tag{5}$$

We can also consider $F(\cdot)$ as the quantile of a normal distribution.

On the other hand, RBDO refers to the optimization scheme where reliability analysis is incorporated into deterministic optimization methods [13]. Herein, reliability is defined as the probability that a system is expected to operate under variations. RBDO approaches exploit stochastic methods to address the statistical nature of constraints and design problems. Given m risk factors, such as deflection, leakage, and local damage, a representative formulation of RBDO reads:

$$\begin{aligned} \min_{\mathbf{x}} \quad & J(\mathbf{x}, \mu_{\boldsymbol{\xi}}) \\ \text{s.t.} \quad & P_j[g_j(\mathbf{x}, \boldsymbol{\xi}) \geq 0] \geq R_j (j = 1, \cdots, m) \end{aligned} \tag{6}$$

where $\mu_{\boldsymbol{\xi}}$ is the mean of the random variable $\boldsymbol{\xi}$, $g_j(\cdot, \cdot)$ denotes the j-th limit-state function that indicates the margin of safety with respect to the j-th risk factor, and R_j is the specified reliability level with respect to the j-th factor. Given the j-th factor, $g_j(\cdot, \cdot) < 0$ and $g_j(\cdot, \cdot) \geq 0$ denote the associated failure region and safe region, respectively.

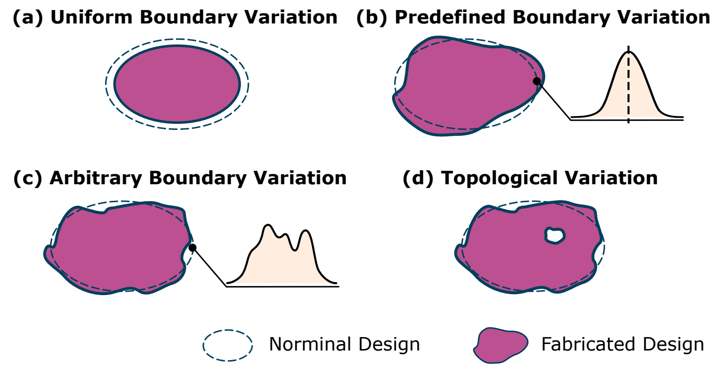

FIGURE 1. Types of geometric uncertainty modeling: (a) Uniform boundary variation where the boundary of the geometry is uniformly "eroded" (*e.g.*, over-etched) or "dilated" (*e.g.*, under-etched) [6, 14, 15]; (b) Predefined boundary variation where the distribution of boundary points is predefined [5]; (c) Arbitrary boundary variation where no assumption is imposed on the distribution of boundary points; (d) Topological variation where the design's topological change (*e.g.*, hole nucleation) is also possible. To the best of our knowledge, past work only considers (a) and (b) when modeling geometric uncertainty, while our proposed method can address "free-form" uncertainties that include all four cases.

Both approaches have been developed for design optimization under geometric uncertainty at various levels of geometric complexity (*i.e.*, size, shape, and topology). Among them, topology optimization under geometric uncertainty has been regarded as highly challenging due to modeling of topological uncertainty, propagation thereof, and stochastic design sensitivity analysis [5]. Previous work either assumes uniform boundary variation [6, 14, 15] (Fig. 1a), imposes predefined distribution on boundary points or material distribution [5, 16] (Fig. 1b). While those methods can simplify geometric uncertainty quantification, the modeled uncertainties do not necessarily conform to realistic scenarios, which usually involve much more complicated geometric variability. For example, in real applications, the boundary variation does not necessarily follow standard distribution (Fig.s 1c) and manufacturing defects do not only happen on the boundary [17] (Fig. 1d). Therefore, how to model "real-world", "free-from" geometric uncertainty without making any simplifying assumption is still an open challenge.

In this work, we overcome this challenge by using a hierarchical deep generative model to learn 1) the underlying distribution of free-form nominal designs and 2) the conditional distribution of fabricated design given any nominal design, under free-form geometric uncertainty (Figures 1c and 1d). We demonstrate the efficacy using two real-world design examples. The ability of modeling free-form geometry and uncertainties allows us to address topological uncertainties.

METHODOLOGY

Let $\mathcal{I}_{\text{nom}}$ and $\mathcal{I}_{\text{fab}}$ denote the datasets of nominal and fabricated designs, respectively:

$$\mathcal{I}_{\text{nom}} = \left\{ \mathbf{x}_{\text{nom}}^{(1)}, ..., \mathbf{x}_{\text{nom}}^{(N)} \right\}$$
$$\mathcal{I}_{\text{fab}} = \left\{ \left(\mathbf{x}_{\text{fab}}^{(1,1)}, ..., \mathbf{x}_{\text{fab}}^{(1,M)} \right), ..., \left(\mathbf{x}_{\text{fab}}^{(N,1)}, ..., \mathbf{x}_{\text{fab}}^{(N,M)} \right) \right\},$$

where $\mathbf{x}_{\text{fab}}^{(i,j)}$ is the j-th realization (fabrication) of the i-th nominal design. The **goals** are to 1) learn a lower-dimensional, compact representation $\mathbf{c}$ of nominal designs to allow accelerated design optimization and 2) learn the conditional distribution $P(\mathbf{x}_{\text{fab}}|\mathbf{c})$ to allow the quantification of manufacturing uncertainty at any given nominal design (represented by $\mathbf{c}$).

To achieve these two goals, we propose a generative adversarial network (Fig. 2a) that enables the hierarchical modeling of nominal designs and fabricated designs. Its generator G generates fabricated designs when feeding in the parent latent vector $\mathbf{c}_p$, the child latent vector $\mathbf{c}_c$, and the noise $\mathbf{z}$; whereas it generates nominal designs simply by using the same generator G but setting $\mathbf{c}_c = \mathbf{0}$. By doing this, we can control the generated nominal designs through $\mathbf{c}_p$ and the generated fabricated designs through $\mathbf{c}_c$. Given the pair of a generated nominal design $G(\mathbf{c}_p, \mathbf{0}, \mathbf{z})$ and a generated fabricated design $G(\mathbf{c}_p, \mathbf{c}_c, \mathbf{z})$, the discriminator D predicts whether the pair is generated or drawn from data (*i.e.*, $\mathcal{I}_{\text{nom}}$ and $\mathcal{I}_{\text{fab}}$). Similar to InfoGAN, we also predict the conditional distribution $Q(\mathbf{c}_p, \mathbf{c}_c|\mathbf{x}_{\text{nom}}, \mathbf{x}_{\text{fab}})$ to promote disentanglement of latent spaces and ensure the latent spaces capture major geometric variability [1]. The GAN is trained using the following loss function:

$$\begin{aligned} \min_{G,Q} \max_{D} \mathbb{E}_{\mathbf{x}_{\text{nom}},\mathbf{x}_{\text{fab}}}[\log D(\mathbf{x}_{\text{nom}}, \mathbf{x}_{\text{fab}})] + \\ \mathbb{E}_{\mathbf{c}_p,\mathbf{c}_c,\mathbf{z}}[\log(1 - D(G(\mathbf{c}_p, \mathbf{0}, \mathbf{z}), G(\mathbf{c}_p, \mathbf{c}_c, \mathbf{z})))] - \\ \lambda \mathbb{E}_{\mathbf{c}_p,\mathbf{c}_c,\mathbf{z}}[\log Q(\mathbf{c}_p, \mathbf{c}_c|G(\mathbf{c}_p, \mathbf{0}, \mathbf{z}), G(\mathbf{c}_p, \mathbf{c}_c, \mathbf{z}))]. \end{aligned} \tag{7}$$

As a result, G decouples the variability of the nominal and the fabricated designs by using $\mathbf{c}_p$ to represent the nominal design (**Goal 1**) and $\mathbf{c}_c$ to represent the fabricated design of any nominal design. By fixing $\mathbf{c}_p$ and sampling from the prior distribution of $\mathbf{c}_c$, we can produce the conditional distribution $P(\mathbf{x}_{\text{fab}}|\mathbf{c}_p) = P(G(\mathbf{c}_p, \mathbf{c}_c, \mathbf{z})|\mathbf{c}_p)$ (**Goal 2**).

Compared to existing uncertainty quantification (UQ) methods, this GAN-based model opens up possibilities of 1) building a universal UQ model compatible with both shape and topological designs, 2) modeling *free-form* geometric uncertainties without the need to make any assumptions on the distribution of geometric variability, and 3) allowing fast prediction of uncertainties for new nominal designs.

The trained generator allows us to sample fabricated designs given any nominal design, simply by sampling the low-dimensional $\mathbf{c}_c$ with a fixed $\mathbf{c}_p$ representing the nominal design (Fig. 2b). We can then evaluate the quantities of interest (QoIs) of these generated fabricated designs using computational (*e.g.*, physics simulation) or experimental methods. The QoIs may include performance, quality, properties, and/or cost. The resulted QoI distribution (*i.e.*, *post-fabrication QoI distribution*) allows us to quantify the uncertainty of QoIs for the nominal design. Note that the proposed framework is agnostic to both the type of designs (*e.g.*, how designs are represented or what geometric variability is presented) and downstream tasks like design optimization and design evaluation. We can integrate the evaluated uncertainty into optimization frameworks such as robust optimization, where we simultaneously optimize the mean QoIs and minimize the influence of uncertainty [11] (Fig. 2c), as well as reliability-based optimization, where we optimize the QoIs subject to constraints such as failure probability or reliability index [13]. The solution is expected to maintain high real-world performance/quality, desired properties, or a low chance of failure even under fabrication imperfection.

RESULTS

We use two real-world robust design examples to demonstrate the effectiveness of our proposed framework. Ideally, to obtain fabricated design data $\mathcal{I}_{\text{fab}}$, we can take the nominal designs from $\mathcal{I}_{\text{nom}}$, fabricate them, and use the actual fabricated designs as data. However, in this study, we simulate the fabrication effects by deforming the geometry of nominal designs based on the following approaches, as a way to save time and cost. Note that how well the simulated manufacturing uncertainty resembles the real-world uncertainty is not central to this proof of concept study. We treat the simulated uncertainty as the real uncertainty only to demonstrate our design under uncertainty framework. In the ideal scenario, we can directly use the real-world fabricated designs to build $\mathcal{I}_{\text{fab}}$ and our proposed framework can still model the fabricated design distribution, since the framework is agnostic to the form of uncertainty. Also note that the required amount of data and latent vector dimensions will depend on the complexity level of geometric variation in data. For example, if the fabricated designs have a higher variation, we may need more fabricated design data and a higher-dimensional child latent vector to maintain the same level of accuracy for modeling the uncertainty.

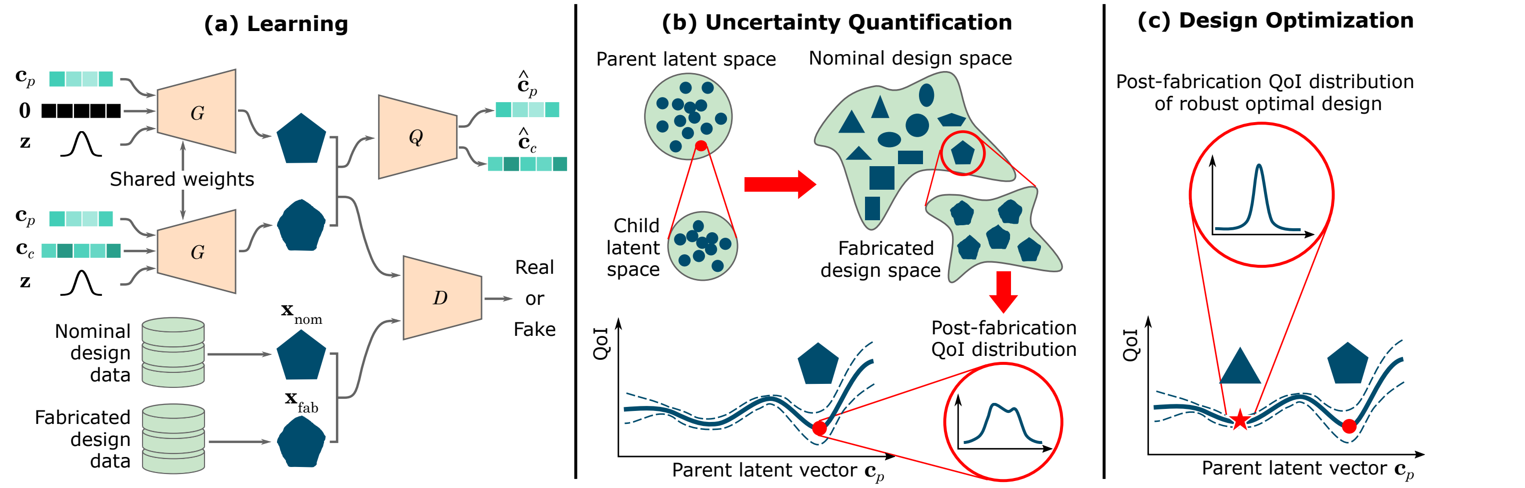

FIGURE 2. Illustration of proposed Generative Adversarial Network-based Design under Uncertainty Framework GAN-DUF: (a) The proposed Hierarchical GAN architecture for simultaneously learning the compact representation of nominal designs and the conditional distributions of fabricated designs; (b) Fabricated designs can be generated by sampling $\mathbf{c}_c$ at any fixed $\mathbf{c}_p$ representing a nominal design. The uncertainty of a nominal design's QoIs can be quantified by evaluating the QoIs of these generated fabricated designs via simulation or experiments; (c) We can optimize $\mathbf{c}_p$ to obtain a nominal design $\mathbf{x}_{\text{nom}}$ with desired post-fabrication QoIs.

Case Study: Airfoil Design

An airfoil is the cross-sectional shape of an airplane wing or a propeller/rotor/turbine blade. The shape of the airfoil determines the aerodynamic performance of a wing or a blade. We use the UIUC airfoil database[1] as our nominal design dataset $\mathcal{I}_{\text{nom}}$. The preprocessing of $\mathcal{I}_{\text{nom}}$ and the creation of the fabricated design dataset $\mathcal{I}_{\text{fab}}$ are described as follows:

Nominal design data. The original UIUC database contains invalid airfoil shapes and the number of surface coordinates representing each airfoil is inconsistent. Therefore, we used the preprocessed data from Chen *et al.* [1] so that outliers are removed and each airfoil is consistently represented by 192 surface points (*i.e.*, $\mathbf{x}_{\text{nom}} \in \mathbb{R}^{192\times 2}$).

Fabricated design data. For airfoil designs, we simulate the effect of manufacturing uncertainty by randomly perturbing the free-form deformation (FFD) control points of each airfoil design from $\mathcal{I}_{\text{nom}}$ [18]. Specifically, the original FFD control points fall on a 3×8 grid and are computed as follows:

$$\mathbf{P}^{l,m}_{\text{nom}} = \left(x^{\min}_{\text{nom}} + \frac{l}{7}(x^{\max}_{\text{nom}} - x^{\min}_{\text{nom}}), y^{\min}_{\text{nom}} + \frac{m}{2}(y^{\max}_{\text{nom}} - y^{\min}_{\text{nom}})\right),$$
$$l = 0,\ldots,7 \text{ and } m = 0,\ldots,2, \tag{8}$$

[1] http://m-selig.ae.illinois.edu/ads/coord_database.html

where $x^{\min}_{\text{nom}}$, $x^{\max}_{\text{nom}}$, $y^{\min}_{\text{nom}}$, and $y^{\max}_{\text{nom}}$ define the 2D minimum bounding box of the design $\mathbf{x}_{\text{nom}}$. To create fabricated designs, we add Gaussian noise $\varepsilon \sim \mathcal{N}(0, 0.02)$ to the y-coordinates of control points except those at the left and the right ends. This results in a set of deformed control points $\{\mathbf{P}^{l,m}_{\text{fab}} | l = 0,\ldots,7; m = 0,\ldots,2\}$. The airfoil shape also deforms with the new control points and is considered as a fabricated design. The surface points of fabricated airfoils are expressed as

$$\mathbf{x}_{\text{fab}}(u,v) = \sum_{l=0}^{7}\sum_{m=0}^{2} B^7_l(u) B^2_m(v) \mathbf{P}^{l,m}_{\text{fab}}, \tag{9}$$

where $0 \le u \le 1$ and $0 \le v \le 1$ are parametric coordinates, and the n-degree Bernstein polynomials $B^n_i(u) = \binom{n}{i} u^i (1-u)^{n-i}$. We set the parametric coordinates based on the surface points of the nominal shape:

$$(\mathbf{u},\mathbf{v}) = \left(\frac{\mathbf{x}_{\text{nom}} - x^{\min}_{\text{nom}}}{x^{\max}_{\text{nom}} - x^{\min}_{\text{nom}}}, \frac{\mathbf{y}_{\text{nom}} - y^{\min}_{\text{nom}}}{y^{\max}_{\text{nom}} - y^{\min}_{\text{nom}}}\right). \tag{10}$$

Perturbing nominal designs via FFD ensures that the deformed (fabricated) shapes are still continuous, which conforms to reality.

The final dataset contains 1,528 nominal designs and 10 fabricated designs per nominal design. Note that since similar nominal designs also have similar fabricated designs, we may need even fewer fabricated designs as training data. Studying the minimum required size of the fabricated design dataset might be interesting future work.

We trained the proposed GAN on $\mathcal{I}_{\text{nom}}$ and $\mathcal{I}_{\text{fab}}$. We set the parent latent vector to have a uniform prior distribution $\mathcal{U}(\mathbf{0},\mathbf{1})$ (so that we can search in a bounded space during the design optimization stage), whereas both the child latent vector and the noise have normal prior distributions $\mathcal{N}(\mathbf{0},0.5\mathbf{I})$. The generator/discriminator architecture and the training configurations were set according to Chen *et al.* [1]. During training, we set both the generator's and the discriminator's learning rate to 0.0001. We trained the model for 20,000 steps with a batch size of 32.

We performed a parametric study to quantify the design space coverage and the uncertainty modeling performance of our trained models under different parent and child latent dimension settings (the noise dimension is fixed to 10). Details on the experimental settings and results are included in Appendix A. Based on the parametric study, we set the parent and the child latent dimensions of 7 and 5, respectively, when performing design optimization.

The objective of the design optimization is to maximize the lift-to-drag ratio C_L/C_D, which is simulated and computed by using the computational fluid dynamics (CFD) solver SU2 [19].

We compared two optimization scenarios:

1. Standard optimization, where we only consider the deterministic performance of the nominal design. The objective is expressed as $\max_{\mathbf{c}_p} f(G(\mathbf{c}_p,\mathbf{0},\mathbf{0}))$.
2. Robust design optimization, which accounts for the performance variation caused by manufacturing uncertainty. The objective is expressed as $\max_{\mathbf{c}_p} Q_\tau\left(f(G(\mathbf{c}_p,\mathbf{c}_c,\mathbf{0}))|\mathbf{c}_p\right)$, where Q_τ denotes the conditional τ-quantile. We set $\tau = 0.05$ in this example.

In each scenario, we performed Bayesian optimization (BO) to find $\mathbf{c}_p$. We evaluate 21 initial samples of $\mathbf{c}_p$ selected by Latin hypercube sampling (LHS) [20] and 119 sequentially selected samples based on BO's acquisition function of expected improvement (EI) [21][2]. In standard optimization, we evaluate the nominal design performance $f(G(\mathbf{c}_p,\mathbf{0},\mathbf{0}))$ at each sampled point. In robust design optimization, we estimate the quantile of fabricated design performances $f(G(\mathbf{c}_p,\mathbf{c}_c,\mathbf{0}))$ by Monte Carlo (MC) sampling using 100 randomly sampled $\mathbf{c}_c \sim P(\mathbf{c}_c)$ at each $\mathbf{c}_p$. Figure 3 shows the optimal solutions and the distributions of ground-truth fabricated design performances[3] of these solutions. By accounting for manufacturing uncertainty, the quantile values of the post-fabrication performance distribution are improved for the robust optimal design $\mathbf{x}^*_{\text{robust}}$, compared to the standard optimal design $\mathbf{x}^*_{\text{std}}$, even though the nominal performance of $\mathbf{x}^*_{\text{robust}}$ is worse than $\mathbf{x}^*_{\text{std}}$. This result illustrates the possibility that the solution discovered by standard optimization can have high nominal performance but is likely to possess low performance when it is fabricated. The robust design optimization enabled by GAN-DUF can avoid this risk.

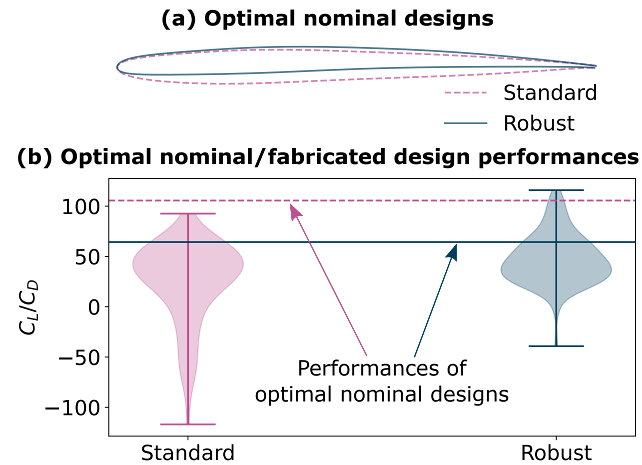

FIGURE 3. Solutions for the airfoil design example: (a) Optimal nominal airfoil designs obtained by standard optimization and robust design optimization; (b) When considering the manufacturing uncertainty, the robust optimal design $\mathbf{x}^*_{\text{robust}}$ shows improved quantile values for the post-fabrication performance distribution compared to the standard optimal design $\mathbf{x}^*_{\text{std}}$, even though the nominal performance of $\mathbf{x}^*_{\text{robust}}$ is slightly worse than $\mathbf{x}^*_{\text{std}}$.

Case Study: Optical Metasurface Absorber Design

Optical metasurfaces are artificially engineered structures that can support exotic light propagation using subwavelength inclusions [22, 23]. Optical metasurface absorbers [24] have applications including medical imaging, sensing, and wireless communications. In this work, the key functionality of interest is large energy absorbance at a range of incident wave frequencies.

We created 1,000 nominal designs and 10 fabricated designs per nominal design (Fig. 5a) by using the following method:

Nominal design data. The nominal design dataset builds on three topological motifs (*i.e.*, I-beam, cross, and square ring) [25, 26]. We create nominal designs by randomly interpolating the signed distance fields of these baselines [27]. As a result, each design is stored as 64×64 level-set values (*i.e.*, $\mathbf{x}_{\text{nom}} \in \mathbb{R}^{64\times 64}$). We can obtain final designs by thresholding the signed distance fields. Building on a given set of baselines, this shape generation scheme allows a unit cell population that is topologically diverse.

Fabricated design data. Similar to the airfoil design example, we randomly perturb a set of 12×12 FFD control points in both x and y directions with white Gaussian noise that has a standard deviation of 1 pixel. This leads to the distortion of the 64×64 grid coordinates at all the pixels, together with the level-set value

[2] The settings of the initial and the total evaluation times in BO are based on the parent latent dimension d_p. Specifically, we performed $3d_p$ initial LHS evaluations and $20d_p$ total evaluations, where $d_p = 7$ as mentioned earlier.

[3] "Ground-truth fabricated design" refers to designs created by the same means by which the designs from $\mathcal{I}_{\text{fab}}$ were created.

at each pixel. We then interpolate a new signed distance field as the fabricated (distorted) design. To account for the limited precision of fabrication, we further apply a Gaussian filter with a standard deviation of 2 to smooth out sharp, non-manufacturable features.

As mentioned in the Background section, optimizing designs with varying topology under geometric uncertainty hosts a great challenge. GAN-DUF can handle this problem by modeling the uncertainty using the proposed generative adversarial network. Same as the airfoil example, we set the parent latent vector to have a uniform prior distribution, while both the child latent vector and the noise have normal prior distributions. Again, we fixed the noise dimension to 10. The generator and the discriminator architectures are shown in Fig. 4. The discriminator predicts both the discriminative distribution $D(\mathbf{x}_{\text{nom}}, \mathbf{x}_{\text{fab}})$ and the auxiliary distribution $Q(\mathbf{c}_p, \mathbf{c}_c | \mathbf{x}_{\text{nom}}, \mathbf{x}_{\text{fab}})$. During training, we set both the generator's and the discriminator's learning rate to 0.0001. We trained the model for 50,000 steps with a batch size of 32.

Figure 5b shows nominal and fabricated designs randomly generated from the trained generator with a parent and a child latent dimensions of 5 and 10, respectively. We performed a similar parametric study, as in the airfoil design example, to quantify the design space coverage of the trained models under varying parent latent dimensions (please see Appendix A for more details).

During the design optimization stage, we set the parent and the child latent dimensions to be 5 and 10, respectively. The objective is to maximize the overall energy absorbance over a range of frequencies. More specifically, a single unit cell of metasurface is made of a dielectric with relative permittivity 2.88-0.09i, where i is the imaginary unit $i = \sqrt{-1}$. The periodic boundary condition is imposed on the boundary of the analysis domain. The performance metric, energy absorbance, is defined as $A(f) = 1 - T(f) = 1 - |S_{11}(f)|^2$, where f is the excitation frequency of an x-polarized incident wave (8-9 THz in this work), T is the transmission, and S_{11} is a component of the S-parameter matrix that characterizes an electrical field intensity in a complex network. To achieve broadband functionality, we formulate the objective function as the sum of energy absorbance at individual frequencies (*i.e.*, $J = \sum_{i=1}^{n_f} A(f_i)$, where n_f is the number of equidistant frequencies at which absorbance is to be observed). The RF Module of COMSOL Multiphysics® [28] is used for evaluation of metasurfaces.

Similar to the airfoil design example, we compared standard optimization with robust design optimization. In each scenario, we performed BO with 15 initial LHS samples and 85 sequentially selected samples based on the acquisition strategy of EI[4].

[4]Same as the airfoil design use case, we performed $3d_p$ initial LHS evaluations and $20d_p$ total evaluations in BO, where $d_p = 5$ is the parent latent dimension.

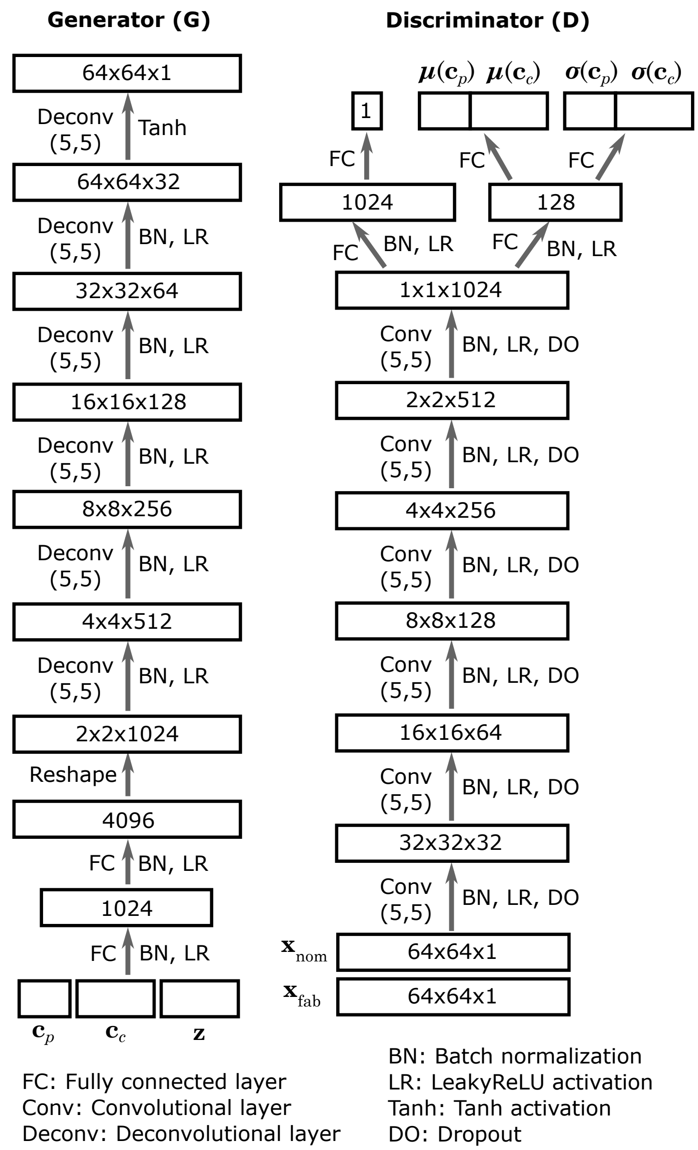

FIGURE 4. Generator and discriminator architectures in the metasurface design example.

The quantile of fabricated design performances at each $\mathbf{c}_p$ was estimated from 20 MC samples. We used fewer MC samples than those in the airfoil design case due to the higher cost of evaluating the objective (*i.e.*, performing wave analysis to compute the energy absorbance). Figure 6 shows the optimal solutions and the distributions of ground-truth fabricated design performances for these solutions. We observe similar patterns as in the airfoil design case, where the standard optimization finds the solution with higher nominal performance, while robust optimization enabled by GAN-DUF finds the solution with higher performances (in general) after fabrication. Note that the effect of robust design

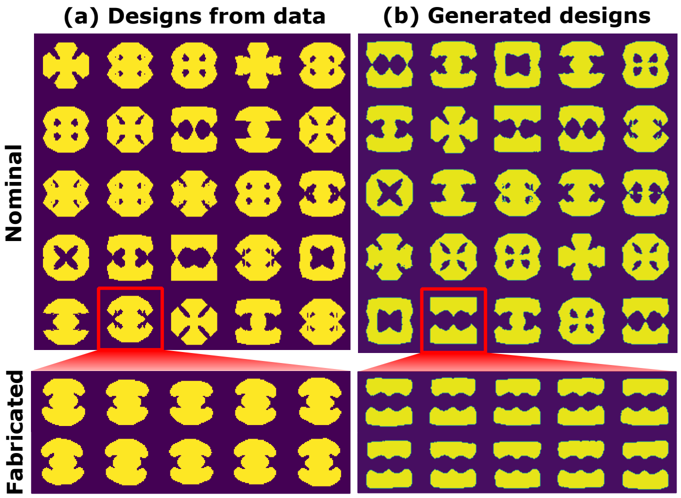

FIGURE 5. Visual inspection on generated designs: (a) Metasurface designs randomly drawn from training data; (b) Designs randomly generated from a trained generator.

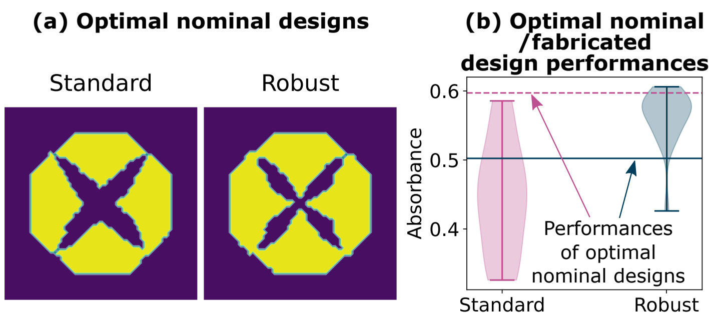

FIGURE 6. Solutions for the metasurface design example: (a) Optimal nominal metasurface designs obtained by standard optimization and robust design optimization; (b) When considering the manufacturing uncertainty, the robust optimal design $\mathbf{x}^*_{\text{robust}}$ shows improved post-fabrication performance distribution compared to the standard optimal design $\mathbf{x}^*_{\text{std}}$, even though the nominal performance of $\mathbf{x}^*_{\text{robust}}$ is worse than $\mathbf{x}^*_{\text{std}}$.

optimization is more significant on metasurface designs (Fig. 6b) than airfoil designs (Fig. 3b), which indicates a difference in the levels of variation in design performance sensitivity to manufacturing uncertainties. This difference can be caused by various factors such as the variance in nominal designs and the physics governing design performances.

CONCLUSION

We proposed GAN-DUF to facilitate design under free-form geometric uncertainty. It contains a novel deep generative model that simultaneously learns a compact representation of nominal designs and the conditional distribution of fabricated designs given any nominal design. The proposed framework is generalizable to any geometric design representations (*i.e.*, both shape and topological designs) and can address free-form uncertainties without the need to make any assumption on the type of uncertainty. We applied GAN-DUF on two real-world engineering design examples (namely shape and topological designs) and showed its capability in finding the design solution that is more likely to possess a better performance after fabrication or manufacturing. Although we only considered fabrication/manufacturing uncertainty when demonstrating the proposed framework, it is also applicable to other sources of geometric uncertainties such as those caused by operational wear or erosion. In addition to robust design optimization demonstrated in this work, we can also combine the proposed hierarchical generative model with reliability-based design optimization to find designs that are unlikely to fail after fabrication or under operational wear/erosion. Built on our preliminary results, as future work, we will 1) perform more tests to quantify GAN-DUF's performance on different design under uncertainty scenarios and 2) use real fabricated designs as training and test data to validate the effectiveness of the GAN-DUF framework in a completely realistic scenario.

ACKNOWLEDGEMENT

This work was supported by the NSF CSSI program (Grant No. OAC 1835782) and the Northwestern McCormick Catalyst Award. We thank the anonymous reviewers for their comments.

REFERENCES

[1] Chen, W., Chiu, K., and Fuge, M. D., 2020. "Airfoil design parameterization and optimization using bézier generative adversarial networks". *AIAA Journal,* ***58***(11), pp. 4723–4735.
[2] Chen, W., and Ramamurthy, A., 2021. "Deep generative model for efficient 3d airfoil parameterization and generation". In AIAA Scitech 2021 Forum, p. 1690.
[3] Chen, W., and Ahmed, F., 2021. "Mo-padgan: Reparameterizing engineering designs for augmented multi-objective optimization". *Applied Soft Computing,* ***113***, p. 107909.
[4] Chen, S., Chen, W., and Lee, S., 2010. "Level set based robust shape and topology optimization under random field uncertainties". *Structural and Multidisciplinary Optimization,* ***41***(4), pp. 507–524.
[5] Chen, S., and Chen, W., 2011. "A new level-set based approach to shape and topology optimization under geometric uncertainty". *Structural and Multidisciplinary Optimization,* ***44***(1), pp. 1–18.
[6] Wang, E. W., Sell, D., Phan, T., and Fan, J. A., 2019. "Ro-

bust design of topology-optimized metasurfaces". *Optical Materials Express,* ***9***(2), pp. 469–482.
[7] Goodfellow, I., Pouget-Abadie, J., Mirza, M., Xu, B., Warde-Farley, D., Ozair, S., Courville, A., and Bengio, Y., 2014. "Generative adversarial nets". In Advances in neural information processing systems, pp. 2672–2680.
[8] Chen, X., Duan, Y., Houthooft, R., Schulman, J., Sutskever, I., and Abbeel, P., 2016. "Infogan: Interpretable representation learning by information maximizing generative adversarial nets". In Advances in Neural Information Processing Systems, pp. 2172–2180.
[9] Du, X., Sudjianto, A., and Chen, W., 2004. "An integrated framework for optimization under uncertainty using inverse reliability strategy". *J. Mech. Des.,* ***126***(4), pp. 562–570.
[10] Maute, K., 2014. "Topology optimization under uncertainty". In *Topology optimization in structural and continuum mechanics*. Springer, pp. 457–471.
[11] Chen, W., Allen, J., Tsui, K.-L., and Mistree, F., 1996. "A procedure for robust design: Minimizing variations caused by noise factors and control factors". *Journal of Mechanical Design, Transactions of the ASME,* ***118***(4), pp. 478–485.
[12] Du, X., and Chen, W., 2004. "Sequential optimization and reliability assessment method for efficient probabilistic design". *J. Mech. Des.,* ***126***(2), pp. 225–233.
[13] Choi, S.-K., Canfield, R. A., and Grandhi, R. V., 2007. *Reliability-Based Structural Optimization*. Springer.
[14] da Silva, G. A., Beck, A. T., and Sigmund, O., 2019. "Stress-constrained topology optimization considering uniform manufacturing uncertainties". *Computer Methods in Applied Mechanics and Engineering,* ***344***, pp. 512–537.
[15] Sigmund, O., 2009. "Manufacturing tolerant topology optimization". *Acta Mechanica Sinica,* ***25***(2), pp. 227–239.
[16] Keshavarzzadeh, V., Fernandez, F., and Tortorelli, D. A., 2017. "Topology optimization under uncertainty via non-intrusive polynomial chaos expansion". *Computer Methods in Applied Mechanics and Engineering,* ***318***, pp. 120–147.
[17] Pham, T., Kwon, P., and Foster, S., 2021. "Additive manufacturing and topology optimization of magnetic materials for electrical machines—a review". *Energies,* ***14***(2), p. 283.
[18] Sederberg, T. W., and Parry, S. R., 1986. "Free-form deformation of solid geometric models". In Proceedings of the 13th annual conference on Computer graphics and interactive techniques, pp. 151–160.
[19] Economon, T. D., Palacios, F., Copeland, S. R., Lukaczyk, T. W., and Alonso, J. J., 2016. "Su2: An open-source suite for multiphysics simulation and design". *Aiaa Journal,* ***54***(3), pp. 828–846.
[20] McKay, M. D., Beckman, R. J., and Conover, W. J., 2000. "A comparison of three methods for selecting values of input variables in the analysis of output from a computer code". *Technometrics,* ***42***(1), pp. 55–61.
[21] Jones, D. R., Schonlau, M., and Welch, W. J., 1998. "Efficient global optimization of expensive black-box functions". *Journal of Global optimization,* ***13***(4), pp. 455–492.
[22] Chen, H.-T., Taylor, A. J., and Yu, N., 2016. "A review of metasurfaces: physics and applications". *Reports on progress in physics,* ***79***(7), p. 076401.
[23] Bukhari, S. S., Vardaxoglou, J. Y., and Whittow, W., 2019. "A metasurfaces review: Definitions and applications". *Applied Sciences,* ***9***(13), p. 2727.
[24] Liu, X., Fan, K., Shadrivov, I. V., and Padilla, W. J., 2017. "Experimental realization of a terahertz all-dielectric metasurface absorber". *Optics express,* ***25***(1), pp. 191–201.
[25] Larouche, S., Tsai, Y.-J., Tyler, T., Jokerst, N. M., and Smith, D. R., 2012. "Infrared metamaterial phase holograms". *Nature materials,* ***11***(5), pp. 450–454.
[26] Azad, A. K., Kort-Kamp, W. J., Sykora, M., Weisse-Bernstein, N. R., Luk, T. S., Taylor, A. J., Dalvit, D. A., and Chen, H.-T., 2016. "Metasurface broadband solar absorber". *Scientific reports,* ***6***(1), pp. 1–6.
[27] Whiting, E. B., Campbell, S. D., Kang, L., and Werner, D. H., 2020. "Meta-atom library generation via an efficient multi-objective shape optimization method". *Optics Express,* ***28***(16), pp. 24229–24242.
[28] Multiphysics, C., 1998. "Introduction to comsol multiphysics®". *COMSOL Multiphysics, Burlington, MA, accessed Feb,* ***9***, p. 2018.

Appendix A: Parametric Study

We conducted parametric studies over parent and child latent dimensions to investigate their effects on the generative performances (we fix the noise dimension to 10). Particularly, we care about two performances: (1) how well the parent latent representation can cover nominal designs, and (2) how well the performance distributions of fabricated designs are approximated. The experimental settings and results are described as follows.

Airfoil Design. We evaluated the first performance (*i.e.*, nominal design coverage) via a fitting test, where we found the parent latent vector that minimizes the Euclidean distance between the generated nominal design and a target nominal design sampled from the dataset (*i.e.*, fitting error). We use SLSQP as the optimizer and set the number of random restarts to 3 times the parent latent dimension. We repeated this fitting test for 100 randomly sampled target designs under each parent latent dimension setting. A parent latent representation with good coverage of the nominal design data will result in low fitting errors for most target designs. Figure 7a indicates that a parent latent dimension of 7 achieves relatively large design coverage (low fitting errors). We evaluated the second performance (*i.e.*, fabricated design per-

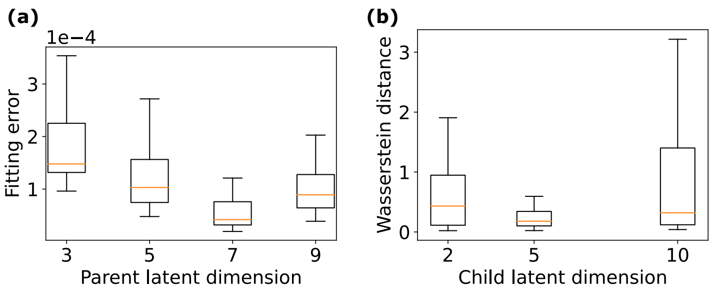

FIGURE 7. Parametric study for the airfoil design example.

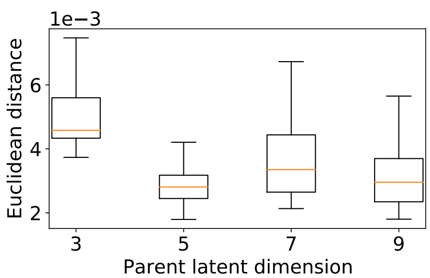

FIGURE 8. Parametric study for the metasurface design example.

formance approximation) by measuring the Wasserstein distance between two conditional distributions — $P(f(\mathbf{x}_{\text{fab}})|\mathbf{x}_{\text{nom}})$ and $P(f(G(\mathbf{c}_p, \mathbf{c}_c, \mathbf{z}))|\mathbf{x}_{\text{nom}})$, where f denotes the objective function. In this example, f is the simulation that computes the lift-to-drag ratio C_L/C_D. For each generated nominal design $\mathbf{x}_{\text{nom}}$, we created 100 "simulated" fabricated designs as $\mathbf{x}_{\text{fab}}$, in the same way we create training data. We also generated the same number of fabricated designs using the trained generator. We compute the Wasserstein distance between these two sets of samples. We repeated this test for 30 randomly generated nominal designs under each child latent dimension setting. Figure 7b shows that when the child latent dimension is 5, we have relatively low Wasserstein distances with the smallest variation (the parent latent dimension was fixed to 7). When the child latent dimension further increases to 10, the uncertainty of the Wasserstein distances increase, possibly due to the higher dimensionality. Note that the training data only contains 10 fabricated designs per nominal design, while at the test phase we use many more samples per nominal design to faithfully approximate the conditional distributions. We do not need that many samples at the training phase because the generative model does not learn independent conditional distributions for each nominal design, but can extract information across all nominal designs.

Optical Metasurface Absorber Design. We performed a fitting test to study the effect of the parent latent dimension on the design space coverage of GANs. Same as in the airfoil design case, we use SLSQP as the optimizer and set the number of random restarts to 3 times the parent latent dimension. Here the fitting error is the Euclidean distance between the signed distance fields of the generated nominal design and a target nominal design sampled from the dataset. Under each parent latent dimension setting, we randomly select 100 target designs. Figure 8 indicates that a parent latent dimension of 5 achieves sufficiently large design coverage, while further increasing the parent latent dimension cannot improve the coverage.